Bifacial PV System Mismatch Loss Estimation and Parameterization

Preprint

Chris Deline[1], Silvana Ayala Pelaez[1], Sara MacAlpine[2], and Carlos Olalla[3]

1 National Renewable Energy Laboratory
2 Juwi Solar Americas
3 Rovira i Virgili University

Presented at the 2019 European PV Solar Energy Conference (EU PVSEC)
Marseille, France
September 9-13, 2019

NREL is a national laboratory of the U.S. Department of Energy
Office of Energy Efficiency & Renewable Energy
Operated by the Alliance for Sustainable Energy, LLC

This report is available at no cost from the National Renewable Energy Laboratory (NREL) at www.nrel.gov/publications.

Contract No. DE-AC36-08GO28308

Conference Paper
NREL/CP-5K00-73541
October 2019

Bifacial PV System Mismatch Loss Estimation and Parameterization

Preprint

Chris Deline[1], Silvana Ayala Pelaez[1], Sara MacAlpine[2], and Carlos Olalla[3]

1 National Renewable Energy Laboratory
2 Juwi Solar Americas
3 Rovira i Virgili University

Suggested Citation
Deline, Chris, Silvana Ayala Pelaez, Sara MacAlpine, and Carlos Olalla. 2019. *Bifacial PV System Mismatch Loss Estimation and Parameterization: Preprint*. Golden, CO: National Renewable Energy Laboratory. NREL/CP-5K00-73541.
https://www.nrel.gov/docs/fy20osti/73541.pdf

NREL is a national laboratory of the U.S. Department of Energy
Office of Energy Efficiency & Renewable Energy
Operated by the Alliance for Sustainable Energy, LLC

This report is available at no cost from the National Renewable Energy Laboratory (NREL) at www.nrel.gov/publications.

Contract No. DE-AC36-08GO28308

Conference Paper
NREL/CP-5K00-73541
October 2019

National Renewable Energy Laboratory
15013 Denver West Parkway
Golden, CO 80401
303-275-3000 • www.nrel.gov

NOTICE

This work was authored in part by the National Renewable Energy Laboratory, operated by Alliance for Sustainable Energy, LLC, for the U.S. Department of Energy (DOE) under Contract No. DE-AC36-08GO28308. Funding provided by U.S. Department of Energy Office of Energy Efficiency and Renewable Energy Solar Energy Technologies Office. The views expressed herein do not necessarily represent the views of the DOE or the U.S. Government. The U.S. Government retains and the publisher, by accepting the article for publication, acknowledges that the U.S. Government retains a nonexclusive, paid-up, irrevocable, worldwide license to publish or reproduce the published form of this work, or allow others to do so, for U.S. Government purposes.

Cover Photos by Dennis Schroeder: (clockwise, left to right) NREL 51934, NREL 45897, NREL 42160, NREL 45891, NREL 48097, NREL 46526.

BIFACIAL PV SYSTEM MISMATCH LOSS ESTIMATION AND PARAMETERIZATION

Chris Deline[1], Silvana Ayala Pelaez[1], Sara MacAlpine[2], Carlos Olalla[3]
[1]National Renewable Energy Laboratory, 15013 Denver West Pkwy, Golden, CO USA
[2]Juwi Solar Americas, 1710 29th St, Boulder, CO USA
[3]Rovira i Virgili University, Dept. of Electrical, Electronic, and Automatic Control Engineering, Tarragona, Spain

ABSTRACT: Non-uniform irradiance on the rear-side of bifacial PV systems can cause additional **mismatch loss** which may not be appropriately captured in PV energy production estimates and software. We have evaluated several **rooftop mounted** systems over high albedo reflective roofs. Mismatch losses of **up to 2% annual loss** for very close-mounted (0.15 m) rooftop systems were found, but losses for high ground-clearance rooftop systems were lower (<0.5%). A simplified empirical relationship was found that links the spatial variation of irradiance (specifically the **mean absolute difference of irradiance)** to the resulting mismatch loss factor, with a R^2 fit better than 0.985. This approximate relationship has been **validated by experiments** on mismatched PV modules, and provides a basis for fast estimation of bifacial mismatch loss factors for use in hourly PV performance simulations such as PVSyst or SAM.
Keywords: bifacial photovoltaics; PV systems

1 INTRODUCTION

Bifacial photovoltaic (PV) system deployments are quickly proliferating due to enhanced production from rear-side irradiance contribution with over 1 GWp cumulative installations worldwide in 2018 [1], [2] and are projected to reach 35% of global market share by 2027 [3]. Bifacial PV modules are sensitive to light incident on both sides, producing additional energy in comparison to monofacial modules [4], [5], thereby reducing the levelized cost of electricity (LCOE) [6], [7].

Bifacial PV makes use of rear irradiance G_{rear}, which depends on mounting conditions such as clearance height, row-to-row spacing, tilt and site's albedo [1], [8]–[10]. Furthermore, the uniformity of G_{rear} along the module plane can be greatly influenced by self-shading of individual modules, and mutual shading of neighboring modules and rows [11]–[13] , not to mention rear racking obstructions [14]. The impact of this nonuniform irradiance is reduction of I_{sc} for individual cells, and thereby non-convex shape to the module I-V curve and reduction in module P_{mp} (Figure 1).

Previous studies have investigated the uniformity of incident light and subsequent mismatch loss of conventional (monofacial) PV systems, which can experience losses due to direct-beam shading [15], [16], and diffuse view-factor shading [17], [18]. In this paper, we specifically look at the influence of rear-incident irradiance, which can be non-uniform throughout the PV module or system and can therefore introduce additional mismatch losses for bifacial PV installations.

The computation of mismatch loss in bifacial systems follows the approach used previously in [19]–[21] for inter-row shading and arbitrary shading of monofacial PV systems. Namely, a detailed cell-level performance model is used to identify the actual array output P_{Array} which includes mismatch losses. This is compared with the ideal output ΣP_{Cells} which is the sum of individual cell-level power excluding mismatch losses. Mismatch loss is therefore calculated by:

$$Mismatch\ loss\% = M[\%] = 1 - \frac{P_{Array}}{\Sigma P_{Cells}} \qquad (1)$$

Although cell-level electrical models are accurate at calculating P_{Array}, the intensive computation time makes them inappropriate for inclusion in fast PV performance models such as PVSyst [22] or SAM [23]. Furthermore, the rear irradiance nonuniformity is a complicated function of ground albedo, clearance height, tilt angle, etc. Therefore a simplified empirical representation of M[%] based only on parameters of irradiance and its spatial distribution would be extremely valuable. This paper describes a reduced-order fit to a series of hourly mismatch factors, based on detailed simulations of multiple bifacial system configurations. This extends previously presented work on bifacial mismatch losses [24] by proposing a universal parameterization of mismatch loss. In particular, M[%] was found in all cases to depend on the spatial distribution of total (front + rear) irradiance for cell i:

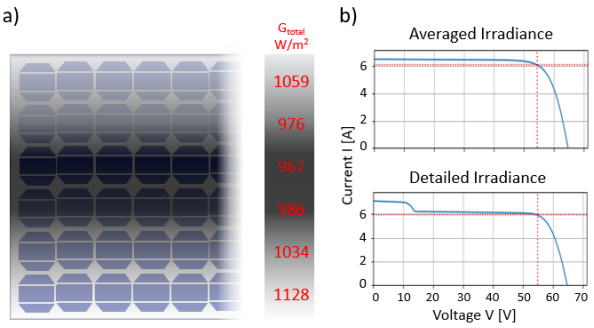

Figure 1: a) Font + rear irradiance distribution of a bifacial module depends on the mounting and site conditions. Example shown for Cairo, June 21st at 2 PM. b) Irradiance mismatch causes additional module loss relative to uniform assumption.

$$G_{total,i} = G_{front,i} + \phi_{Bifi}\, G_{rear,i} \qquad (2)$$

where ϕ_{Bifi} is the module's bifaciality. In particular, two scalar representations of irradiance distribution were found to have high correlation with M[%] over multiple system configurations – the standard deviation of $G_{total,i}$ and the Mean Absolute Difference of $G_{total,i}$. These are represented in relative terms by dividing by average total irradiance:

$$\sigma[\%] = \frac{1}{\bar{G}_{total}} \sqrt{\frac{\Sigma\left(G_{total,i} - \bar{G}_{total}\right)^2}{n-1}} \qquad (3)$$

$$\Delta[\%] = \frac{1}{n^2 \bar{G}_{total}} \sum_{i=1}^{n} \sum_{j=1}^{n} \left| G_{total,i} - G_{total,j} \right| \quad (4)$$

The Mean Absolute Difference in (4) has been shown to apply more accurately for non-normal distributions [25] which we have also found to be the case here.

2 ELECTRICAL AND OPTICAL MODEL DETAILS

2.1 Single-cell electrical models

The cell-level simulations of bifacial modules have been carried out with a modified version of the tool presented in [20] following the method of [26]. In brief, to account for the characteristics of bifacial modules, each cell's equivalent combined rear and front irradiance $G_{total,i}$ depends on the row position i. The detailed cell-level modeling uses the 5-parameters equivalent model of the cells, as described in [27].

2.2 Bifacial optical simulations

Front and rear irradiance values for use in the full cell-level model are given by annual simulations with a previously described bifacial view-factor model [28], [29] which has been validated against other rear irradiance models and field data in [10]. In this paper, G_{front} and G_{rear} are obtained hourly across the tilted plane of a semi-infinite array, simulating a fixed-tilt rooftop system. A high-reflective white rooftop of 0.62 albedo was considered, with GCR of 0.67 and tilt of 10°. Four ground clearance heights are modeled, between 0.15 m and 1 m

PV module electrical characteristics are based on a 350W, 72-cell n-PERT module with ϕ_{Bifi} = 0.9. Annual hourly simulations are conducted for multiple typical-year climate conditions for each system scenario. A typical US climate (Richmond, VA) along with a sunny (Cairo, Egypt) and cloudy (Shanghai, China) climate are included.

3 SIMULATION RESULTS AND REDUCED-ORDER MODEL

The total annual mismatch loss for the high albedo rooftop system is shown in Fig. 2 with varying ground clearance heights. Mismatch loss M[%] based on Eq. (1) is the total annual system power lost due to front and rear irradiance nonuniformity. There is a strong dependence on ground clearance height H, which is expected because rear irradiance nonuniformity increases at low H [12]. There is also a climate dependence, with cloudy conditions such as in Shanghai reducing the times of high DNI reflected irradiance which gives rise to the irradiance nonuniformity.

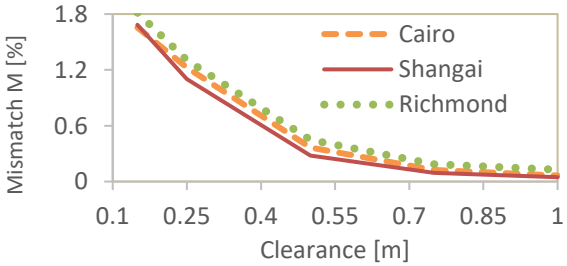

Figure 2: Annual mismatch loss M[%] for cloudy and sunny climates, for different clearance heights of a low-tilt bifacial rooftop array.

Total annual mismatch loss for the rooftop scenario ranges from 1.85% for the Cairo low ground clearance condition to less than 0.1% for the Shanghai 1 m ground clearance condition. These values are in the same range as was previously reported in [24] for similar fixed-tilt conditions.

3.1 Reduced-Order Model Development

The annual results of Fig. 2 indicate relatively low overall mismatch loss, particularly for high clearance height conditions. However individual hourly mismatch loss values can be much higher - in excess of 10%. By looking at hourly mismatch loss as a function of irradiance standard deviation and mean absolute difference from (3) and (4), we can identify consistent performance trends.

The hourly annual simulation data for the location of Richmond, VA for the four different ground clearances are compiled and considered together. Data with low irradiance ($G_{Front} < 100$ Wm^{-2}or $G_{Rear} < 15$ Wm^{-2}) are excluded, leaving 13,000 remaining hourly points. Initial analysis shown in Fig. 3 indicates that when mismatch loss M[%] is compared with standard deviation of total irradiance σ[%], Eq (3), the data seems to fall into two populations. Data with relatively low mismatch (grey points in Fig. 3) happen during typical solar azimuth within 90° of south when the sun is in front of the array plane. However, higher mismatch conditions result when the sun is behind the plane of the array (black points in Fig. 3, solar azimuth >90° from south) and direct shading can occur.

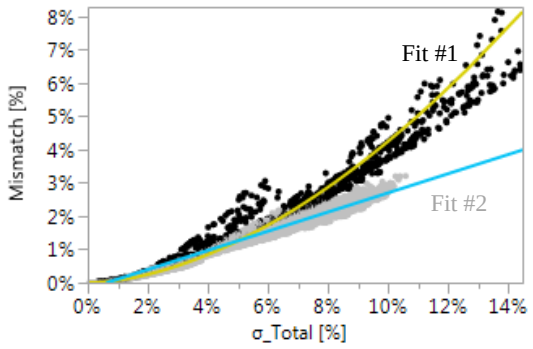

Figure 3: Hourly simulation showing mismatch M[%] as a function of G_{total} standard deviation. Log-log Fit #1 shown for high solar angle (azimuth > 90° from south) data, black. Linear Fit #2 shown for daytime data (grey).

The population of high-mismatch data is best represented by a log-log fit with the following empirical parameters:

$$M[\%]_{Fit1} = e^{1.067 + 1.82 * \ln(\sigma[\%])} \quad (5)$$

The remaining lower-mismatch data comprise the majority (> 90%) of points, and are best approximated by a linear trend:

$$M[\%]_{Fit2} = -0.002 + 0.29 * \sigma[\%] \quad (6)$$

Log-log Fit #1 is shown in Fig. 3 through the high solar angle data (black), and linear Fit #2 is shown through the low incidence angle data (grey).

3.2 Reduced Order Model – Mean Absolute Difference

The fact that the data of Fig. 3 divides into two populations, each fit by a different trendline may indicate that Eq (3) is not the most appropriate way to describe these irradiance distributions. Standard deviation is typically used to describe normal populations, and the rear irradiance distribution is not necessarily normally distributed. The use of mean absolute difference Eq. (4) can be used for non-normal distributions more effectively [25]. Indeed, Eq. (4) does result in a single population of data regardless of solar azimuth angle (Fig. 4). This data is fit to a high degree of accuracy ($R^2 > 0.985$) with a 2nd-degree fit:

$$M[\%]_{Fit3} = 0.12\,\Delta[\%] + 2.77\,\Delta[\%]^2 \qquad (7)$$

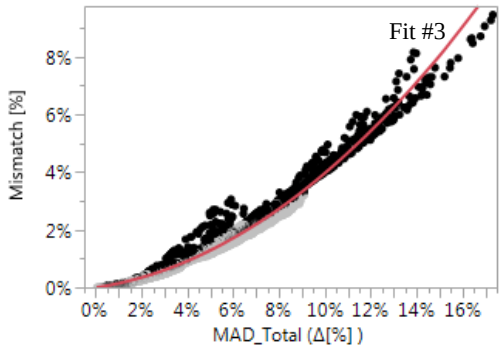

Figure 4: Hourly simulation showing mismatch M[%] as a function of G_{total} Mean Absolute Difference along with Fit #3 (Eq. 7).

Table I: Annual Mismatch loss simulated by the complete model vs the reduced order model

Clearance	*Full model*	*Fit #1 (Eq. 5)*	*Fit #2 (Eq. 6)*	*Fit #3 (Eq. 7)*
0.15m	1.86%	1.62%	1.71%	1.81%
0.25m	1.37%	1.24%	1.36%	1.34%
0.5m	0.49%	0.45%	0.55%	0.49%
1m	0.15%	0.00%	0.12%	0.11%
Avg M[%] *ERROR*	N/A	+/- 0.12	+/- 0.06	+/- 0.04

The three empirical fits given by Eq. 5, 6 and 7 are then used to create estimates of overall annual mismatch loss for each scenario by totaling the hourly mismatch power lost. This is compared with the annual results of the full model for the Richmond VA climate shown in Fig. 2. This indicates the degree of increased error by moving from a detailed model to a simple empirical one. The results in Table I indicate that the empirical fits are relatively good for annual cumulative mismatch estimation. In particular, Fit #2 and #3 have an accuracy of better than 0.1% for annual mismatch loss.

4 EXPERIMENTAL VALIDATION

Reliance on modeled data is insufficient to give confidence in our empirical model's ability to describe field conditions. IV curve measurements of PV modules were collected under artificially applied mismatch conditions to verify the applicability of these models to more general conditions.

Unlike previously published experiments such as [30] or [31] where a large amount of opaque shading is applied to cells, the amount of mismatch considered here is quite modest. Previous experiments have shown the response of PV systems to partial shading to be significant and non-linear. However for bifacial systems, the irradiance mismatch is not likely to result in cell reverse bias or bypass-diode turn-on. This is because regardless the amount of rear shadowing or inherent mismatch on the back of the module, G_{front} will be much more uniform and greater in magnitude than G_{rear}.

4.1 Experiment configuration

Here the effect of irradiance mismatch was investigated experimentally on PV modules with small amounts of artificial partial shading applied. A Spire 4600 long-pulse flash IV curve simulator was used, along with two Siemens SM55 36-cell monocrystalline modules (mono-facial). Each SM55 module has two junction boxes – one on each end of the module- which house the module's bypass diodes and interconnect terminals. In addition, each module also has ribbon tabs accessible, allowing each group of 12 cells to be individually contacted. By placing the two SM55 modules side by side on the flash simulator and connecting the module terminals in series, the end result is a single 72-cell series of monocrystalline cells, in which every 12 cells can be individually contacted and measured, and the entire series connection can be measured.

The class AAA rating of the Spire simulator indicates that irradiance spatial uniformity is within 2% when no artificial shading is applied. To introduce artificial irradiance mismatch, a series of semi-transparent films are used, with spectrally normalized transparency between %T = 84% (3M CG3300) and %T = 90% (3M CG6000). After an initial baseline measurement with no artificial shading applied, five additional test configurations are applied with increasing levels of shading. The final two measurement conditions utilize multiple layers of transparency film to achieve higher amounts of shading loss. The amount of shading film applied to each module sub-string is given in Table II. To minimize ambiguous results and multiple IV curve peaks, the shading is applied uniformly across an entire row of 12 cells. Mismatch loss *M*[%] from Eq. 1 is calculated by comparing the module power at its terminals with the sum of each 12-cell substring power. 4-wire measurement is used to remove interconnection series losses, which would accumulate over 6 separate sub-string measurement.

Table II: Filter transparency %T applied to module substrings for each test condition

Test#	*M1 str1*	*M1 str2*	*M1 str3*	*M2 str1*	*M2 str2*	*M2 str3*
0	N/A	N/A	N/A	N/A	N/A	N/A
1	90%	N/A	84%	N/A	N/A	N/A
2	90%	N/A	84%	N/A	N/A	90%
3	90%	75%	84%	N/A	N/A	90%
4	90%	75%	84%	70%	N/A	90%
5	64%	75%	84%	70%	N/A	90%

N/A : no artificial shading applied.

The standard deviation and MAD for total irradiance is not calculated directly, but inferred from the measured I_{sc} of each of the six sub-strings. Some inherent mismatch in the modules is visible from the 1.5% standard deviation in I_{sc} from the no-shading Test 0 case. Other measured I_{sc} values for each of the other shading tests are shown in Fig. 5. Calculated I_{sc} standard deviation and MAD have similar values, and range up to 18% for the most extensive shade condition. Note that Fig. 5 is ordered by most extensively shaded substring for each test condition, not necessarily consistently from one test to the next.

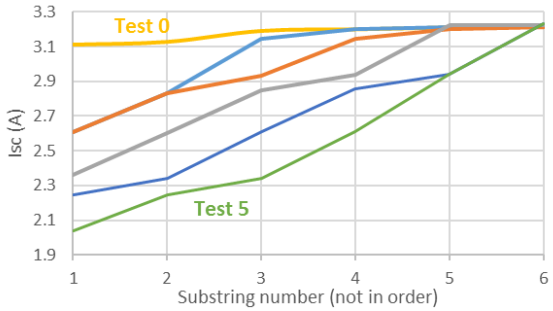

Figure 5: Measured substring I_{sc} for each of the shading tests. I_{sc} standard deviation and Mean Absolute Difference each vary from 1.5% - 18%

4.2 Experiment Results

The measured mismatch loss due to nonuniform shading of the modules is shown in Fig. 6, along with the empirical models of Eq. 5 and Eq. 7 which match the experimental data within experimental uncertainty.

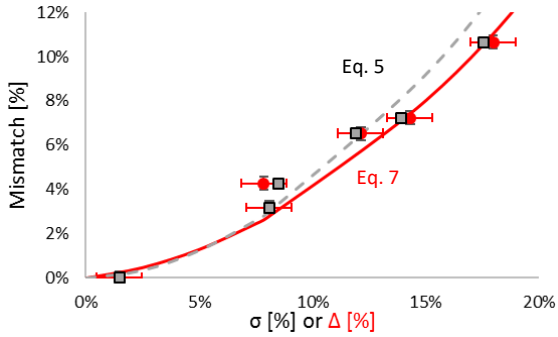

Figure 6: Measured mismatch loss *M*[%] for each of the shading tests plotted vs I_{sc} standard deviation (black squares) or I_{sc} MAD (red circles) which have similar value in this experiment. Empirical models from Eq. 5 and Eq. 7 shown for comparison.

It is interesting to note that the logarithmic Fit #1 (Eq. 5) has a better fit to this experimental data than the linear Fit #2 (Eq. 6, not shown), which greatly under-estimates mismatch loss. However, based on Table I, for expected field bifacial conditions Fit #2 provides the better match. This is likely related to the fact that Fit #1 has better accuracy for large amounts of mismatch loss, while Fit #2 is the most accurate at small levels of mismatch. By parameterizing the irradiance by MAD and using Fit #3 however, accuracy is maintained at large and small amounts of mismatch loss.

An expanded version of this work [32] includes the present methodology applied to various 1-axis tracked systems, including end-of-row brightening and the presence of rear shading obstructions, each of which increase mismatch losses [33].

ACKNOWLEDGEMENTS

This work was authored, in part, by the National Renewable Energy Laboratory, operated by Alliance for Sustainable Energy, LLC, for the U.S. Department of Energy (DOE) under Contract No. DE-AC36-08GO28308. Funding was provided by the U.S. Department of Energy's Office of Energy Efficiency and Renewable Energy (EERE) under Solar Energy Technologies Office (SETO) Agreement Numbers 30286 and 34910. The views expressed in the article do not necessarily represent the views of the DOE or the U.S. Government. A portion of the research was performed using computational resources sponsored by the Department of Energy's Office of Energy Efficiency and Renewable Energy and located at the National Renewable Energy Laboratory.

REFERENCES

[1] J. Libal and R. Kopecek, *Bifacial photovoltaics : technology, applications and economics.*, no. Vol. 107. Stevenage: The Institution of Engineering and Technology, 2018.

[2] R. Kopecek and J. Libal, "Towards large-scale deployment of bifacial photovoltaics," *Nat. Energy*, vol. 3, no. 6, p. 443, 2018.

[3] "International Technology Roadmap for Photovoltaic (ITRPV) results 2017 including maturity report 2018, 9th Edition, September 2018," 2018.

[4] A. Cuevas, A. Luque, J. Eguren, and J. del Alamo, "50% more output power from an albedo-collecting flat panel using bifacial solar cells," *Sol. Energy*, vol. 29, no. 5, pp. 419–420, 1982.

[5] X. Sun, M. R. Khan, C. Deline, and M. A. Alam, "Optimization and performance of bifacial solar modules: A global perspective," *Appl. Energy*, vol. 212, no. September 2017, pp. 1601–1610, 2018.

[6] S. B. Darling, F. You, T. Veselka, and A. Velosa, "Assumptions and the levelized cost of energy for photovoltaics," *Energy Environ. Sci.*, vol. 4, no. 9, pp. 3133–3139, 2011.

[7] M. Bazilian *et al.*, "Re-considering the economics of photovoltaic power," *Renew. Energy*, vol. 53, pp. 329–338, 2013.

[8] U. A. Yusufoglu, T. M. Pletzer, L. J. Koduvelikulathu, C. Comparotto, R. Kopecek, and H. Kurz, "Analysis of the annual performance of bifacial modules and optimization methods," *IEEE J. Photovoltaics*, vol. 5, no. 1, pp. 320–328, 2015.

[9] T. S. Liang *et al.*, "A review of crystalline silicon bifacial photovoltaic performance characterization and simulation," *Energy Environ. Sci.*, vol. 12, pp. 116–148, 2019.

[10] S. Ayala Pelaez, C. Deline, S. Macalpine, B. Marion, J. S. Stein, and R. K. Kostuk, "Comparison of bifacial solar irradiance model predictions with field validation," *IEEE J. Photovoltaics*, vol. 9, no. 1, pp. 82–88, 2019.

[11] L. Kreinin, N. Bordin, A. Karsenty, A. Drori, D. Grobgeld, and N. Eisenberg, "PV module power gain due to bifacial design. Preliminary experimental and

simulation data," in *35th IEEE Photovoltaic Specialists Conference*, 2010, pp. 002171–002175.
[12] C. Deline, S. MacAlpine, B. Marion, F. Toor, A. Asgharzadeh, and J. S. Stein, "Assessment of bifacial photovoltaic module power rating methodologies—inside and out," *IEEE J. Photovoltaics*, vol. 7, no. 2, pp. 575–580, 2017.
[13] A. Lindsay *et al.*, "Modelling of single-axis tracking gain for bifacial PV systems," in *32nd European Photovoltaic Solar Energy Conference and Exhibition, Munich, Germany*, 2016, pp. 1610–1617.
[14] S. Ayala Pelaez, C. Deline, P. Greenberg, J. S. Stein, and R. K. Kostuk, "Model and validation of single-axis tracking with bifacial PV," *IEEE J. Photovoltaics*, vol. 9, no. 3, pp. 715–721, 2019.
[15] A. Woyte, J. Nijs, and R. Belmans, "Partial shadowing of photovoltaic arrays with different system configurations: literature review and field test results," *Sol. energy*, vol. 74, no. 3, pp. 217–233, 2003.
[16] E. Karatepe, M. Boztepe, and M. Colak, "Development of a suitable model for characterizing photovoltaic arrays with shaded solar cells," *Sol. Energy*, vol. 81, no. 8, pp. 977–992, 2007.
[17] D. Passias and B. Källbäck, "Shading effects in rows of solar cell panels," *Sol. Cells*, vol. 11, no. 3, pp. 281–291, 1984.
[18] M. Van Schalkwijk, A. J. Kil, and T. C. J. Van Der Weiden, "Dependence of diffuse light blocking on the ground cover ratio for stationary PV arrays," *Sol. energy*, vol. 61, no. 6, pp. 381–387, 1997.
[19] C. Deline, A. Dobos, S. Janzou, J. Meydbray, and M. Donovan, "A simplified model of uniform shading in large photovoltaic arrays," *Sol. Energy*, vol. 96, pp. 274–282, 2013.
[20] C. Olalla, D. Clement, D. Maksimović, and C. Deline, "A cell-level photovoltaic model for high-granularity simulations," in *15th European Conference on Power Electronics and Applications (EPE), Lille, France*, 2013, pp. 1–10.
[21] S. MacAlpine, C. Deline, and A. Dobos, "Measured and estimated performance of a fleet of shaded photovoltaic systems with string and module-level inverters," *Prog. Photovoltaics Res. Appl.*, vol. 25, no. 8, pp. 714–726, 2017.
[22] B. Wittmer and A. Mermoud, "Yield simulations for horizontal axis trackers with bifacial PV modules in PVSyst," in *35th European Photovoltaic Solar Energy Conference and Exhibition, Brussels, Belgium*, 2018.
[23] N. Blair *et al.*, "System advisor model, sam 2014.1. 14: General description," National Renewable Energy Laboratory Golden, CO, 2014.
[24] R. Bailey and J. Jaubert, "A simplified method to approximate bifacial system mismatch losses," in *5th Bifi PV Workshop, Denver, Colorado*, 2018, no. August.
[25] S. Yitzhaki, "Gini's mean difference: a superior measure of variability for non-normal distributions," *Metron*, vol. 61, no. 2, pp. 285–316, 2003.
[26] V. Quaschning and R. Hanitsch, "Numerical simulation of current-voltage characteristics of photovoltaic systems with shaded solar cells," *Sol. energy*, vol. 56, no. 6, pp. 513–520, 1996.
[27] J. P. Singh, A. G. Aberle, and T. M. Walsh, "Electrical characterization method for bifacial photovoltaic modules," *Sol. Energy Mater. Sol. Cells*, vol. 127, pp. 136–142, 2014.
[28] B. Marion *et al.*, "A practical irradiance model for bifacial PV modules," in *44th IEEE Photovoltaic Specialist Conference (PVSC), Washington, DC.*, 2017.
[29] NREL, "bifacialVF." GitHub, 2019.
[30] M. C. Alonso-Garcia, J. M. Ruiz, and F. Chenlo, "Experimental study of mismatch and shading effects in the I-V characteristic of a photovoltaic module," *Sol. Energy Mater. Sol. Cells*, vol. 90, no. 3, pp. 329–340, 2006.
[31] K. Sinapis *et al.*, "A comprehensive study on partial shading response of c-Si modules and yield modeling of string inverter and module level power electronics," *Sol. Energy*, vol. 135, pp. 731–741, 2016.
[32] C. Deline, S. Ayala Pelaez, S. Macalpine, and C. Olalla, "Estimating and parameterizing mismatch power loss in bifacial photovoltaic systems," *(Submitted)*, 2019.
[33] S. Ayala Pelaez, C. Deline, J. S. Stein, B. Marion, K. Anderson, and M. Muller, "Effect of torque-tube parameters on rear-irradiance and rear-shading loss for bifacial PV performance on single-axis tracking systems," in *46th IEEE Photovoltaic Specialists Conference proceedings, Chicago IL*, 2019.